CHEMMEDCHEM

CHEMISTRY ENABLING DRUG DISCOVERY

Accepted Article

Title: Design, synthesis, and dual evaluation of novel quinoline and quinolinium iodide salt derivatives as potential anticancer and antibacterial agents

Authors: Guofan Jin, Fuyan Xiao, Zhenwang Li, Xueyong Qi, Lei Zhao, and Xianyu Sun

To be cited as: *ChemMedChem* 10.1002/cmdc.202000002

Link to VoR: http://dx.doi.org/10.1002/cmdc.202000002

A Journal of

ChemPubSoc Europe

WILEY-VCH

www.chemmedchem.org

WILEY-VCH

FULL PAPER

Design, synthesis, and dual evaluation of novel quinoline and quinolinium iodide salt derivatives as potential anticancer and antibacterial agents

Guofan Jin[a]*, Fuyan Xiao[a], Zhenwang Li[b], Xueyong Qi[a], Lei Zhao[c] and Xianyu Sun[b]*

[a] Pro. G.F Jin, Dr. X. Y. Qi, F. Y. Xiao
School of Pharmacy
Jiangsu University
Zhenjiang 212013, China
E-mail: 1000004770@ujs.edu.cn
[b] Pro. X. Y. Sun, Z. W. Li
College of Animal Science and Technique
Bayi Agriculture University
Daqing 163319, Heilongjiang, China
E-mail: sxianyu@163.com
[c] Dr. L. Zhao
Siping Institute for food and Drug Control
Siping 136000, China

Supporting information for this article is given via a link at the end of the document.

Abstract: A series of novel quinoline and quinolinium iodide derivatives were designed and synthesized to discover potential anticancer and antibacterial agents. All of the active structure compounds were identified by nuclear magnetic resonance (NMR), such as ^{1}H-NMR, ^{13}C-NMR, infrared radiation (IR), high resolution mass spectrometry (HR-MS) and Carlo Erba Instruments CHNS-O EA1108 spectra analysis. With regard to the anticancer properties, the in vitro cytotoxicity against three human cancer cell lines (A-549, Hela and SGC-7901) were evaluated. The antibacterial properties against two human bacterial strains, *Escherichia coli* (ATCC 29213) and *Staphylococcus aureus* (ATCC 8739), along with minimum inhibitory concentration (MIC) values were evaluated. The target alkyliodine substituted compounds, exhibited significant antitumor and antibacterial activity, of which compound 8-((4-(benzyloxy)phenyl)amino)-7-(ethoxycarbonyl)-5-propyl-[1,3]dioxolo[4,5-g]quinolin-5-ium (**12**) was found to be the most potent derivative with IC_{50} values of 4.45±0.88, 4.74±0.42, 14.54±1.96, and 32.12±3.66 against A-549, Hela, SGC-7901, and L-02 cells, respectively, stronger than the positive control 5-FU and MTX. Furthermore, compound **12** had the most potent bacterial inhibitory activity. The MIC of this compound against *Escherichia coli* (ATCC 29213) and *Staphylococcus aureus* (ATCC 8739) was 3.125 nmol·mL^{-1}, which was smaller than that of the reference agents, amoxicillin and ciprofloxacin.

Introduction

Cancer and infections are the most serious problems that need to be solved. With the continuous improvement of human health requirements, research and development of new drugs has accelerated.[1] The existing drugs are no longer sufficient for a variety of refractory diseases, which requires further improvement of longer-term effective comprehensive drugs.[2-6]

Cancer is a disease that is difficult to cure; it exhibits abnormal metabolic processes in living organisms for a variety of reasons, mainly due to various features,[7-10] such as complexity, diversification, and continuity. In many studies reported in recent years, a strategy to increase the apoptosis activity has been proposed,[11-14] and it was considered to be a potential cancer treatment method. This is a programmed cellular suicide process that removes damaged cells from multicellular organisms at the cellular level that is inactivated.[15, 16] Quinoline compounds can induce and regulate some transcription factors to mediate apoptosis and metabolism, and inhibit the occurrence of cancer and tumors. In addition, quinoline compounds have been confirmed in related studies, which can be effective in inhibiting the development and progression of cancer and tumors.[17-21]

On the other hand, infectious diseases recently have faced major challenges in the world. The number of people with various plagues and deaths has increased considerably. Therefore, the direction of developing new broad-spectrum antibacterial drugs is also more diversified, trended, and comprehensive.[22-25] This is reflected mainly in the structural modification of existing antibiotics, the improvement of the antibacterial spectrum, the reduction of side effects, and the tendency to overcome and contain drug resistance. Thiazolidinone and quinolones are the most commonly used synthetic antibacterial drugs since 2014,[26-28] and their antibacterial spectrum is Gram-positive and Gram-negative bacteria. The structural uniqueness of quinoline is not only used widely in energy, agriculture, organic luminescent materials,[29, 30] etc., but also plays an important role in medicine, including antibacterial,[31] anti-cancer,[32] anti-tumor,[33] and anti-HIV.[34] Quinoline is a specific inhibitor of bacteria type II topoisomerase, namely DNA gyrase.[35-40] The compounds have potential anticancer and antitumor effects owing to the structural similarity between the two gyrase enzymes.

Based on the development of comprehensive drugs, such as cancer and viral infections at home and abroad,[41,42] this group has attempted to modify the active target of quinoline, i.e., an iodoalkyl chain was introduced into the nitrogen in the auto-assembly zone of the 1st position. The introduction of a hydrophilic aromatic cyclic amine onto the carbonyl group at the 4-position, in which DNA is combined, helped improve the water solubility as well as the anti-cancer and anti-proliferative effects in vitro.

Results and Discussion

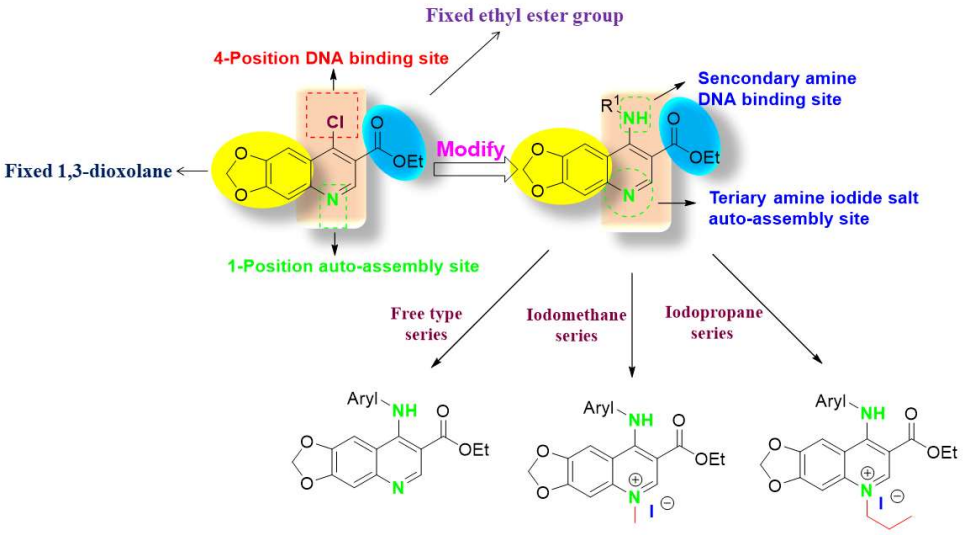

Figure 1. Schematic diagram of the overall design of quinoline derivatives.

Design

According to existing reports, most studies have focused on the synthesis of new quinolones. The overall aims of the authors were to design new quinoline and quinoliunium iodine salt derivatives based on the important structural features of DNA gyrase.[43,44] The candidate structure was designed to take hydrophobic or hydrophilic aryl rings and / or quaternary amine salt moieties linked to the quinoline core at the 1- and 4-positions. Based on retaining the quinoline core, an attempt was made to modify the 1- and 4- positions. The 1, 3-dioxolane base of the quinoline core itself is a very important structure-effect group, and the water-soluble and activity of the ethyl ester group on the entire structure cannot be ignored. First, the carbonyl group at the 1-position is often an important part of the hydrogen bond energy level with DNA. The oxygen atom is converted to a secondary amine to increase the binding energy to DNA. In addition, the introduction of an arylamine can increase the lipophilic amine and the external protein increased the π-H hydrogen bonding ability. Second, the Schiff base tertiary amine drugs of the 4-position are a dynamic self-assembly area. To optimize the auto-assembly activity, methyl iodide and iodine propane were introduced, and their conversion to quaternary ammonium salts to facilitate the positively and negatively charged differential induction of an auto-assembled superstructure were examined. Finally, different designs of quinoline and quinoline iodide salts were proposed to examine their effects on the anticancer and antibacterial dual activities. These drugs are also used widely in many anticancer and antibacterial studies because of the similar heterocyclic iodide structure.[45,46] The synthesis of the target compound was carried out according to the outlined synthetic scheme, and the anticancer and antibacterial activities of the derivative were evaluated. Among them, quinoline was selected as the starting structure for further optimization for the following reasons: 1) a simple method to synthesize the chemical structure and develop a series of novel quinoline derivatives; 2) from the docking result (Fig-2) showing quinolone 4-position aromatic amine or aryl ether, the NH group or aryl-O-aryl interacts with the catalytic residue through hydrogen bonding (H-bond); and 3) for the first proposed method, the concept of auto-assembly effects of drug-aggregation induced by multi-aromatic iodine quaternary ammonium salt (Fig-1).

The docking result suggested there were several key interactions between the 4-position and Human topoisomerase I, among which two key H-bonds were formed between the NH group or aryl-O-aryl interacts with the catalytic residue of DG 112 and LYS 425, respectively.

Chemistry

The novel 7-(ethoxycarbonyl)-8-(arylamino)-[1,3]dioxolo[4,5-g]quinolin-5-ium iodide derivatives were synthesized according to Scheme-1. Ethyl-8-chloro-[1,3]dioxolo[4,5-g]quinoline-7-carboxylate[47] intermediate was prepared by the condensation of malonic acid with the corresponding reagent in the presence of the condition through a four step process. The reaction of the intermediate with benzylamine in anhydrous acetonitrile under reflux overnight resulted in the ethyl 8-(aryl)-[1,3]dioxolo[4,5-g]quinolone -7-carboxylate derivatives 1~4. The iodination of 1, 2, 3, and 4 with an excess of iodomethane or iodopropane under reflux provided the target compounds, 5-12, in moderate yield. The chemical structures of all the synthesized new compounds were characterized by ^{1}H NMR, ^{13}C NMR, IR, HRMS, and CHNS-O EA1108.

The IR spectrum showed a strong band at 1470-1485 cm^{-1} due to quaternary amine groups in addition to a band at 1400-1500 cm^{-1} assigned to the amine of iodine salt. The ^{1}H NMR spectrum revealed the presence of blunt singlet signals assigned to the -NH- proton at 8.84-10.36 ppm, -N-CH- at 8.95-9.10 ppm, and O-CH_2-O at 6.08-6.10 ppm for two protons. In contrast, iodoalkane substituted derivatives -NH- proton at 10.27-11.59 ppm, the -N^{+}-CH- at 9.07-9.38 ppm, and O-CH_2-O at 6.18-6.29 ppm, respectively. The ^{13}C NMR spectra indicated the ketone functional groups: the presence of singlet signals at 165.9-168.2 ppm corresponding to C=O carbons, and alkane iodine salt singlet signals at 10.0-15.0 ppm.

Biology

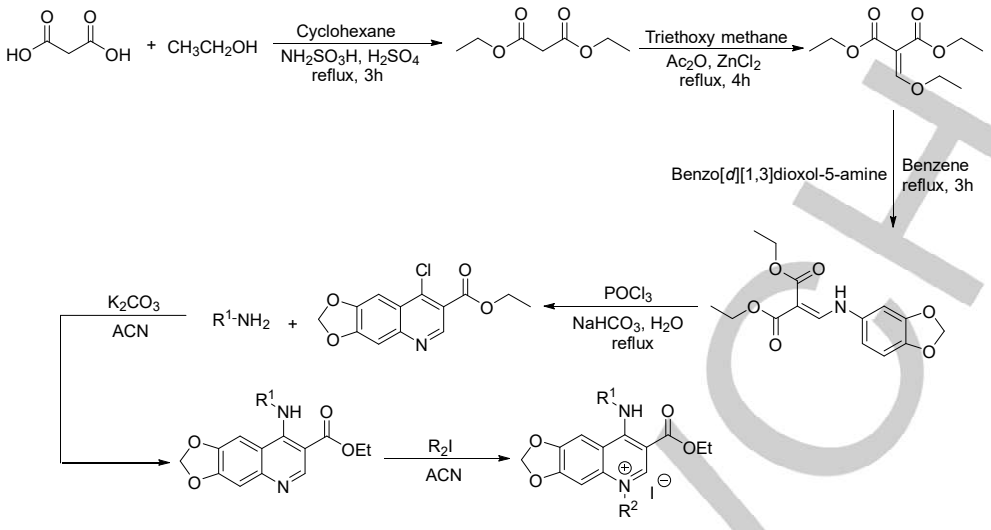

1 R^1 = -CH_2CH_2Ph

2 R^1 = -$CH_2CH_2Ph(OCH_3)_2$

3 R^1 = -CH_2Ph

4 R^1 = -$PhOCH_2Ph$

5 R^1 = -CH_2CH_2Ph; R^2 = -CH_3

6 R^1 = -$CH_2CH_2Ph(OCH_3)_2$; R^2 = -CH_3

7 R^1 = -CH_2Ph; R^2 = -CH_3

8 R^1 = -$PhOCH_2Ph$; R^2 = -CH_3

9 R^1 = -CH_2CH_2Ph; R^2 = -$CH_2CH_2CH_3$

10 R^1 = -$CH_2CH_2Ph(OCH_3)_2$; R^2 = -$CH_2CH_2CH_3$

11 R^1 = -CH_2Ph; R^2 = -$CH_2CH_2CH_3$

12 R^1 = -$PhOCH_2Ph$; R^2 = -$CH_2CH_2CH_3$

Scheme 1. General synthetic route of quinoline derivatives.

Table 1. In vitro growth inhibitory activity (IC50μM) of compounds 1-12 against human lung cancer cell line (A549), human hela cell line (HeLa), human gastric carcinoma cell line (SGC-7901), normal hepatocyte cell line (L02) and normal lung cell line (IMR-90) by the MTT assay.

	Compounds		IC_{50}				
	R^1	R^2	A549	Hela	SGC-7901	L-02	IMR-90
1	-CH_2CH_2Ph	-	31±6.25	73±6.55	>120	>200	>200
2	-$CH_2CH_2Ph(OCH_3)_2$	-	94±4.63	73±4.83	>120	>200	>200
3	-CH_2Ph	-	46±18.96	>120	>120	>200	>200
4	-$PhOCH_2Ph$	-	17±0.95	>120	>120	>200	>200
5	-CH_2CH_2Ph	-CH_3	54±5.39	36±0.98	89±1.80	139±13.60	>200
6	-$CH_2CH_2Ph(OCH_3)_2$	-CH_3	>120	>120	114±1.81	>200	>200
7	-CH_2Ph	-CH_3	49±5.42	30±2.06	74±4.99	125±9.67	182±27.66
8	-$PhOCH_2Ph$	-CH_3	47±8.39	45±14.13	85±11.62	124±8.45	173±22.49
9	-CH_2CH_2Ph	-$CH_2CH_2CH_3$	55±4.58	44±3.95	89±2.89	127±9.58	169±15.28
10	-$CH_2CH_2Ph(OCH_3)_2$	-$CH_2CH_2CH_3$	>120	>120	>120	>200	>200
11	-CH_2Ph	-$CH_2CH_2CH_3$	38±7.32	39±1.82	92±2.76	121±15.18	>200
12	-$PhOCH_2Ph$	-$CH_2CH_2CH_3$	4.4±0.88	4.7±0.42	14±1.96	32±3.66	109±10.17
5-FU	-	-	98±0.72	109±2.81	113±1.07	>200	>200
MTX	-	-	60±9.14	107±1.97	84±7.47	18±13.10	>200

IC_{50}: Each value was averaged by three parallel groups of eight repeats and calculated using a SigmaPlot software.

Evaluation of cytotoxicity activity in vitro

Compounds **1-12** were assessed for their anti-proliferative activity in five cell lines, namely the human lung cancer cell line (A549), human hela cell line (HeLa), human gastric carcinoma cell line (SGC-7901), normal liver L-02 cell line (L02) and nomal lung cell line (IMR-90) by MTT (3-(4,5-dimethylthiazol-2-yl) -2,5-diphenyltetrazolium bromide) assay.[48-53] The anticancer drug 5-FU (5-fluoro-2,4(1H, 3H)pyrimidinedione) and MTX (methotrexate) were co-assayed as the positive control. All compounds tested were dissolved in DMSO and then diluted by the culture medium before the treatment of cultured cells.

All synthesized 1- and 4-substituted ethyl-8-arylamino-[1,3]dioxolo[4,5-g]quinoline-7-carboxylate and ethyl-8-arylamino-[1,3]dioxolo[4,5-g]quinoliniumiodoalkyl-7-carboxylate derivatives were tested on the human cancer cell lines; the data is listed in Table-1 and the fitted curved is showed in Figure S-16.

Compared to the non-substituted iodoalkane compounds, all acquired compounds with iodoalkane substitution at the 1-position (**7**, **8**, **11**, and **12**) showed significantly improved potency. Regarding substitution at the 4-position on ethyl-8-arylamino- [1,3]dioxolo[4,5-g]quinoline-7-carboxylate, the effects of the aromatic ring appeared to have low activities. This is because the substitution of the 4-position into the bulky-aromatic ring leads to blocking of docking site of NH and DNA which affects the activity of the compound considerably (**1~4**). Therefore, the introduction of branched chains in the aromatic ring site was to alleviate steric hindrance, but the effect was still not satisfied, and unsatisfactory results were obtained (IC_{50} > 120). In addition, on the normal hepatocyte cell line (L02) and normal lung cell line (IMR 90), IC_{50} values (>200 μM) clearly indicated that the compounds had the same potency as the reference drug 5-FU.

Regarding the various R^2, the pyridine ring with an alkyl-iodine substituted at the para-position (**5~12**) exhibited better potency than non-substituted position (**1~4**). The para-substituted pyridine ring with a methyl (**8**) or propygroup (**12**) appeared to contribute concurrently to the potency. In contrast to the other analogs, **12** with aromatic ether substitution at R^1 also demonstrated good enzymatic potency. To explore the binding modes of the ethyl-8-arylamino-[1,3]dioxolo[4,5-g]quinoliniumiodoalkyl- 7-carboxylate, one of the most active inhibitors **12** was selected as a representative and docked to the crystal structure of human topoisomerase I (PDB: 1TL8). The docking of **12** in Fig. 3a displayed a free energy of the binding affinity of -9.3 kcal/mol. The 3D binding model of compound **12** in the binding site of the enzyme displayed mainly hydrogen bond acceptor interactions through the oxygen of benzodioxoles with TPC11, between the carbonyl oxygen and base DA113, between the oxygen of arylamine and amino acid residue Lys425, and hydrogen bond donor interaction between the N at the 4-position and base DG112. The compound also displayed π-π interactions of arylamine-substituted group and DG112, and CH-π interactions of arylamine-substituted group and base DA113. The binding mode also displayed other hydrophobic and cation interactions. Molecular docking is an intuitive way to preliminarily simulate the binding of compound **12** to the action site. And these intensive interactions make it a robust combination with Top I which was thought to be the target of quinoline in the effect of anticancer. Thus, the reason for obvious efficacy of **12** was explicated from another perspective by the binding mode.

According to the above analysis, compound **12** exhibited significant growth inhibition with an IC_{50} of 4.4±0.88, 4.7±0.42, and 14±1.96 against A-549, Hela, and SGC-7901, respectively.

Evaluation of antibacterial activity in vitro

The newly synthesized compound **1-12**, were evaluated for their antibacterial activity by determining the MIC against *Escherichia coli* (ATCC 29213) and *Staphylococcus aureus* (ATCC 8739). The test compounds dissolved in DMSO were added to the culture medium (brain heart infusion for *S. mutans* and Müller-Hinton agar for other bacteria) to obtain final concentrations of 1-50 nmol mL^{-1}. A standardized suspension of the test bacterium was inoculated and incubated for 24-48 h at 37 °C, and the lowest concentration of the compounds that prevented the development of visible growth was then analyzed by calculating the minimal inhibitory concentrations (MIC values). Ciprofloxacin and amoxicillin were used as controls and assayed under identical conditions. All experiments were performed in triplicate.

In general, all compounds exhibited promising antibacterial activity against the bacterial strains tested in comparison with the reference drugs. Compounds **7**, **8**, **11**, and **12** showed eight~four times higher antibacterial activity against *E. coli* than ammoxicillin and ciprofloxacin with MIC values of 6.25~3.125 nmol/mL. In addition, these compounds also showed eight~four times higher antibacterial activity against *S. aureus* than amoxicillin and ciprofloxacin with MIC values of 6.25~3.125 μg/mL. In conclusion, compounds **7**, **8**, **11**, and **12** showed higher antibacterial activity against *E. coli* and *S. aureus* to that of amoxiicillin and ciprofloxacin. In particular, compound 12 showed excellent antibacterial activity. Nevertheless, compounds (**1~4**) did not show obvious activity compared to the reference drug (Table-2).

Lipophilicity

Lipophilicity is a major physico-chemical parameter to consider in drug design. This property has a considerable impact on in vivo pharmacokinetic parameters as well on the drug efficacy. A proper lipo-solubility of drugs to make it possible to pass through the biofilm, and a well-turned water-solubility is expected to facilitate the humoral transport of the drug. N-octanol/water partition coefficient (i.e., ClogP) was calculated on ACD/Labs website.

Compound **1~12** were investigated for their lipophilicity as well and the data is shown in table-2. Compound 5~12 alkyliodine substituted at the 1-position in pyridine with the 4-position N-phenyl substituent showed quite different result on N-octanol/water partition coefficient by comparing to unsubstituted **1~4**. By considering the substituted at 1-position **5~12**, it appears that iodomethyl group series and iodopropane group showed exactly different trend. In the series of **5~8**, methy iodine substitution at 1-position shows the decreased logP values, as observed by comparing **1** (unsustitution, logP = 2.53) to **5** (methy iodine, logP = 2.27), **2** (unsustitution, logP = 1.56) to **6** (methy iodine, logP = 1.22), **3** (unsustitution, logP = 2.18) to **7** (methy iodine, logP = 1.97), and **4** (unsustitution, logP = 2.09) to **8** (methy iodine, logP = 1.88).

On the contrary, replacement of a methyl substituent by a iodopropane group leads to higher molecular weight compounds, with significantly higher ClogP values. Indeed, for **9~12**, a series of substituents with an iodopropane group, ClogP values was getting higher, by comparing with their respective previous compounds **1~4**.

Derivatives **1~4** are preliminary compounds constitute by quinoline, and with a 4-position N-phenyl substituent on the pyridine ring. The influence of the nature of the 4-position N substitute group on the lipophilicity of quinolines was also studied. By comparing four quinolines **1~4**, it appears that the substitution by none oxygen group showed higher ClogP values. Thus, the presence of an oxygen atom directly influences the lipophilicity of the studied compounds, it may explain the weak contribution in global molecular lipophilicity.

Structure-activity relationship (SAR)

Based on the SAR studies and from the obtained biological results, the un-substituted **1~4** did not exhibit potential anticancer and antibacterial activities. In contrast, **5~12** alkyliodine substituted at the 1-position in pyridine with the 4-position *N*-phenyl substituent possessed the highest dual activity against all cancer cell and strains tested. The alkyliodine substituents at the 1-position was introduced, such as iodomethyl group in **7** and **8** with iodopropane group in **11** and **12**, respectively, containing an iodine quaternary ammonium salt group, and the anticancer activity against some cancer cells was more significant than that of 5-FU and MTX. Moreover, the antibacterial activity against certain strains showed higher activity compared to amoxicillin and ciprofloxacin.

The conversion of a 4-position carbonyl group to a hydrophobic aromatic amine group to obtain **1~4** compounds, and most of these structures contained a hydrophobic group, and had little effect on the activity of the cancer cells and strains. Accordingly, iodoalkyl was introduced further to obtain **5~12** compounds. Among these compounds, compounds **7** and **8** with **11** and **12** exhibiting extremely high activity in terms of double inhibition. On the other hand, other iodo quaternary ammonium salt derivatives were not as strong as expected, and only had a general inhibitory effect on cancer cells and strains, such as compounds **5** and **6** with **9** and **10**, respectively. In particularly, **6** and **10** showed the weak inhibitory to cancer cell lines (>120 to A549, Hela), which were substituted at 4-position by methoxy-phenethylamine. Besides the hindrance effect by bulky-aromatic group, this can also be interpreted by the low lipophilicity (i.e., ClogP, Table-2) which may bring about the low cell membrane permeability, thereby, influenced the effectiveness of the derivatives. Although iodomethane and iodopropane were introduced at the same 1-position, and aromatic groups were introduced at the 4-position, the activities exhibited by them were different greatly.

This type of decrease in activity may due be to the large space conformation, hindered space combined with enzyme-binding pocket conflict, or that the 4-position aromatic amine group hinders the ability to combine with the DNA.

Among all the derivatives containing an iodo quaternary ammonium salt group, the compounds substituted at the 1- and 4-positions all exhibited extremely high dual activity. Preliminary synthetic SAR studies have shown that to obtain better dual activity, the 1-position on the mother structure should contain odd-numbered atoms in chain of hydrophobic groups and the 4-position should include hydrophobic aromatic amine groups to have a positive impact on the structure of dual activity.[54,55]

Table 2. Antibacterial screening in terms of the MIC (μg/mL**)** for the tested compounds in reference to Amoxicillin and Ciprofloxacin, respectively.

Compound			MIC[a] / (nmol.mL-1)		ClogP[b]
	R^1	R^2	*Escherichia coli*	*Staphylococcus aureus*	
1	$-CH_2CH_2Ph$	-	> 50	> 50	2.53
2	$-CH_2CH_2Ph(OCH_3)_2$	-	25	50	1.56
3	$-CH_2Ph$	-	> 50	25	2.18
4	$-PhOCH_2Ph$	-	6.25	6.25	2.09
5	$-CH_2CH_2Ph$	$-CH_3$	25	12.5	2.27
6	$-CH_2CH_2Ph(OCH_3)_2$	$-CH_3$	12.5	6.25	1.22
7	$-CH_2Ph$	$-CH_3$	6.25	12.5	1.97
8	$-PhOCH_2Ph$	$-CH_3$	6.25	3.125	1.88
9	$-CH_2CH_2Ph$	$-CH_2CH_2CH_3$	50	50	2.89
10	$-CH_2CH_2Ph(OCH_3)_2$	$-CH_2CH_2CH_3$	6.25	25	2.11
11	$-CH_2Ph$	$-CH_2CH_2CH_3$	6.25	6.25	2.85
12	$-PhOCH_2Ph$	$-CH_2CH_2CH_3$	3.125	3.125	2.67
Amoxicillin	-	-	50	25	
Ciprofloxacin	-	-	25	12.5	

[a] MIC (minimum inhibitory concentration) values represent the average of three readings; [b] calculated on ACD/Labs website.

Molecular docking study

AutoDock Vina 1.1.2. software was used to perform docking simulations.[56,57] In the present study, the derivatives were designed based on the quinoline core, depending on the former studies on the mechanism of anticancer and antibacterial activity. The 3D crystal structure of human topoisomerase I and *S. aureus* DNA gyrase (Topo II) reported in Protein Data Bank (PDB) were used as the receptor for docking studies (PDB ID: 1TL8, 2XCT).[58-62] The co-crystallized structure of the target proteins were downloaded from the PDB and prepared for docking using the docking program AutoDockVina 1.1.2. and MGLTools. The docking result was analyzed and optimized by Pymol 1.5.6. (Fig-2).

The other two compounds were docked as comparative objects. The 3D ligand interactions of the combination in Fig. 2a showed the binding pattern of selected derivative **7** to Human DNA topoisomerase I in the covalent complex with a 22 base pair DNA duplexprotein (PDB ID: 1TL8). The docking of **7** displayed a free energy of the binding affinity of -9.6 kcal/mol. Compound **7** exhibited one hydrogen bond acceptor interaction between the carbonyl oxygen of ester group and TPC11 in addition to the ionic interactions with the amino acid residues Arg364, Lys425, Lys436, and Lys532. Moreover, compound **7** also exhibited π-π interactions of quinolone pyridine ring with base DT10, DA113, and TPC11 in addition to π-π stacking interactions between the quinoline benzene ring and TPC11, arylamine phenzene and base DG112, respectively. These π-π stacking interactions make a significant contribution to stabilizing the docking structure.

The docking of **7** in Fig. 2b (DNA gyrase) displayed a free energy of the binding affinity of -8.1 kcal/mol. Compound **7** exhibited hydrogen bond acceptor interactions between the oxygen of benzodioxoles and base DC12, and the hydrogen bond donor interaction between N at the 4-

position and base DG9. In addition, π-π stacking interactions occur between the quinolone pyridine ring and two bases DA13 or DG9 in addition to π-π interactions of the quinolone phenyl ring and base DA13, DC12. The π-π interaction also existed in the arylamine phenyl ring and base DT8, in addition to the cation-π interaction of the arylamine phenyl ring and amino acid residue Arg458.

The anticancer docking of 11 in Fig. 2c displayed the free energy of the binding affinity of -9.5 kcal/mol. As shown in Fig. 2c, the 3D ligand interactions of compound **11** showed π-π interactions not only between the pyridine ring and base DA113 or DT10 or TPC11, but also the π-π stacking interactions of quinoline benzene ring and TPC or DT10, as well as between arylamine phenzene and base DG112. Compound **11** also displayed a hydrogen bond acceptor interaction of the carbonyl oxygen of ester group and TPC11 in addition to ionic interactions with the amino acid residues, Arg364, Lys425, Lys436 and Lys532.

Antibacterial docking of **11** in Fig. 2d displayed a free energy of the binding affinity of -8.1 kcal/mol. Docking of compound **11** displayed mainly π-π interactions between the pyridine ring, quinoline benzene ring, and base DA13 and DG9 in addition to arylamine phenzene and amino acid residues Arg458. In addition, the hydrogen bond acceptor interaction between the oxygen of benzodioxoles and base DC12 in addition to the cation-π interaction of arylamine phenzene and amino acid residue Arg1122 were noted.

The docking of **12** in Fig. 2e displayed a free energy of the binding affinity of -9.3 kcal/mol. In contrast, the docking of compound **12** displayed hydrogen bond acceptor interactions mainly between the oxygen of benzodioxoles and TPC11, between the carbonyl oxygen and base DA113, between the oxygen of arylamine and amino acid residue Lys425, hydrogen bond donor interaction between N at the 4-position and base DG112. In addition, compound **12** displayed π-π interactions of arylamine-substituted group and DG112, in addition to CH-π interactions of the arylamine-substituted group and base DA113.

The binding mode also displayed other hydrophobic and cation interactions. Docking of **12** in Fig. 2f displayed a free energy of the binding affinity of -9.4 kcal/mol. Compound **12** displayed CH-π interactions mainly between the arylamine-substituted group and base DA13 or DG9 in addition to other CH-π interactions of quinoline benzene ring and amino acid residue Phe1123. It also displayed hydrogen bond acceptor between carbonyl oxygen and base DA13, π-π interaction between quinoline pyridine ring and base DT8, besides cation-π interactions of amino acid residues Arg1122, Arg458 and quinoline core, arylamine-substituted group, respectively.

The scores of all the affinity scores caculated by molecular docking software are listed in the Table-3. According to the table, compounds **7**, **11** and **12** have acceptable values to match the good inhibitory activities on the proliferation of cancer cells, with the scores are in the range of - 9.6 ~ - 9.3. However, the level of scoring is not the only criterion to judge the combining abilit. In addition, various interactions are also the reasons for the robust binding with the receptor. For example, the presentence of four hydrogen bonds in the conjugate of compound **12** and enzyme makes the binding site more stable, thus, inhibitory activity of compound **12** is the most prominent.

Conclusions

A series of arylamine-substituted iodo quaternary amine embedded quinolone derivatives were synthesized. Coupling of the aryamine functional groups produced the target compounds, the iodo quaternary amine could be further substituted to produce the final compound in moderate yield. To lay the foundation for the subsequent development of pharmacological toxicology with better novel quinoline compounds, and design and synthesize a series of new quinoline derivatives with iodoalkyl and arylamine groups at the 1- and 4-positions of the functional side chain, new quinoline and quinolinium iodine salt derivatives were prepared, in addition, their anticancer and antibacterial effects were studied as well. It is showed that the 1-position substituted compounds had salient activity comparing to unsubstituted one. The relationship between the structure activity and molecular docking was also evaluated with derivatives as new comprehensive drugs. The effects of introducing functional groups, and the importance and specificity of the odd substituted chains on the overall structure activity were examined. This study confirmed that the compounds with odd atoms in substituted chains at 4-position firmly showed dual activity. Nevertheless, more follow-up research will be needed.

Experimental Section

Materials and Methods

All solvents and reagents were commercially purchased and used as received and employed further purification. Moisture-sensitive reactions were performed under nitrogen atmosphere. Dichloromethane and acetonitrile were distilled over calcium hydride. All glassware including needles and syringes were torch flame or oven-dried and kept in a desiccator before use. The reaction products were isolated and purified by column chromatography (silica gel 200~230 mesh). Thin-layer chromatography (TLC) was used to monitor the progress of the reaction. Analysis of TLC results at 254 nm and 360 nm wavelengths under UV lamps. Characterization of the products at each stage by NMR spectroscopy, ^{1}H, and ^{13}C NMR spectra were recorded on Bruker Avance II spectrometer in $CDCl_3$ (400 MHz for ^{1}H and100 MHz for ^{13}C); chemical shifts are expressed in ppm, versus internal tetramethylsilane (TMS) = 0 for ^{1}H and ^{13}C. Coupling constants (*J*) are given in Hz. Elemental analyses were performed using a Carlo Erba Instruments CHNS-O EA1108 analyser. IR spectra of samples were recorded on a Nicolet avato-370 FT-IR analyzer using KBr disks. Carlo Erba Instruments CHNS-O EA1108 analyser and HR-MS (FAB) (Jeol LTD JMS-HX 110/110A) were performed by the Chosun University of the Republic of Korea.

General Procedure for the Synthesis of 1-4

Ethyl 8-chloro-[1,3]dioxolo[4,5-g]quinoline-7- carboxylate (1.0 eq.) was added to a solution of the arylamine compound (2.5 eq.) in dry acetonitrile (10 mL) and stirred at 80°C for 8-10 h. Thin layer chromatography was used to monitor the progress of the reaction. The solvent was added to 10 mL water with 5 mL dichloromethane and extracted 3 times. The organic layer was dried anhydrous magnesium sulfate and filtered. The residue was purified by column chromatography (EtOAc:petroleum ether = 1:8) to produce a yellowish solid.

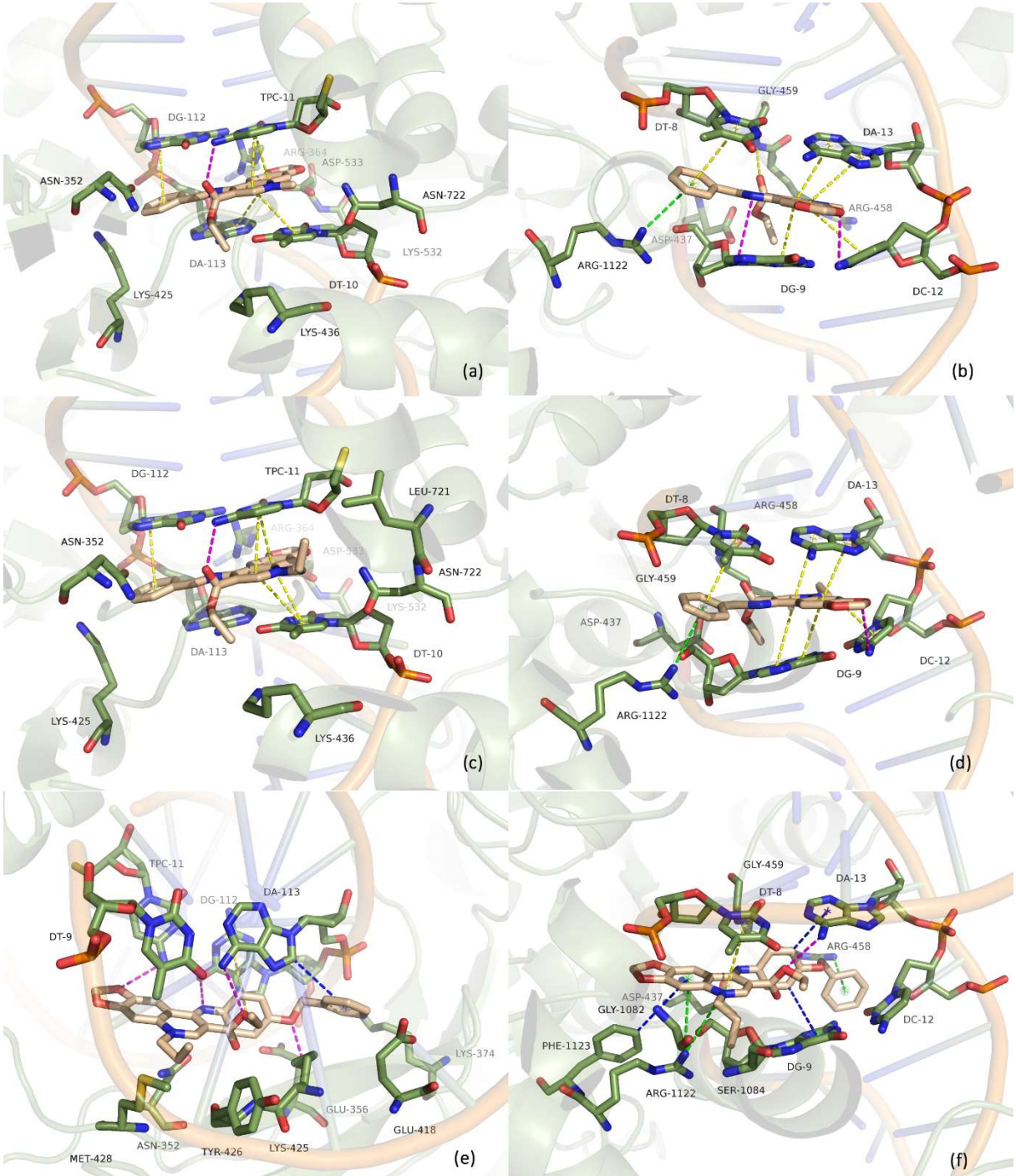

Figure 2. 3D binding mode of derivatives **7**, **11** and **12** in the binding site of Human topoisomerase I (PDB ID: 1TL8; a, c and e) and *S. aureus* DNA gyrase (Topo II, PDB ID: 2XCT; b, d and f).

Table 3. Docking score obtained for compounds **7**, **11** and **12**.

PDB code	Entry	Affinity score (kcal·mol^{-1})	Interaction with receptor
1TL8	7	-9.6	DT 10, DA 113, DG 112, TPC 11, ARG 364, LYS 425, LYS 436, LYS 532.
	11	-9.5	DT 10, DA 113, DG 112, TPC 11, ARG 364, LYS 425, LYS 436, LYS 532.
	12	-9.3	DA 113, DG 112, TPC 11, LYS 425.
2XCT	7	-8.1	DA 13, DG 9, DC 12, DT 8, ARG 458.
	11	-8.1	DA 13, DG 9, DC 12, ARG 1122, ARG 458.
	12	-9.4	DA 13, DT 8, DG 13, ARG 1122, ARG 458, PHE 1123.

Ethyl 8-(phenethylamino)-[1,3]dioxolo[4,5-g]quinoline-7-carboxylate 1

A yellow solid (1.1 g, 84.8%): ^{1}H NMR (400MHz, $CDCl_3$, ppm): *δ* 8.96 (s, 1H), 8.87 (s, 1H,), 7.47 (s, 1H), 7.33–7.25 (m, 6H), 6.10 (s, 2H), 4.40–4.37 (m, 2H), 3.97 (m, 2H), 3.05–3.01 (t, *J* = 7.2Hz, 7.6Hz, 2H), 1.44–1.40 (t, *J* = 7.2Hz, 3H). ^{13}C NMR (100MHz, $CDCl_3$, ppm): *δ* 168.6, 156.4, 151.2, 150.0, 149.6, 146.0, 138.1, 128.8, 128.6, 126.8, 115.0, 106.7, 104.0, 102.0, 101.9, 60.6, 50.7, 37.6, 14.4.

Ethyl 8-((3,4-dimethoxyphenethyl)amino)-[1,3]dioxolo[4,5-g]quinoline-7-carbox ylate 2

A yellowish solid (1.3 g, 85.0%): ^{1}H NMR (400MHz, $CDCl_3$, ppm): *δ* 8.95 (s, 1H), 7.50 (s, 1H), 7.32–7.28 (m, 2H), 6.85–6.81 (m, 3H), 6.11 (s, 2H), 4.37–4.34 (m, 2H), 3.97–3.96 (d, *J* = 5.2 Hz, 2H), 3.90–3.88 (d, *J* = 6.8 Hz, 6H), 3.00–2.96 (t, *J* = 7.2Hz, 2H), 1.43–1.40 (t, *J* = 7.2Hz, 3H). ^{13}C NMR (100MHz, $CDCl_3$, ppm): *δ* 166.6, 156.4, 151.3, 149.0, 147.9, 146.0, 130.7, 120.7, 115.0, 112.3, 111.5, 106.7, 103.8, 102.1, 102.0, 60.6, 55.9, 55.8, 50.9, 37.2, 14.3.

Ethyl 8-(benzylamino)-[1,3]dioxolo[4,5-g]quinoline-7-carboxylate 3

A yellowish solid (1.0 g, 79.2%): ^{1}H NMR (400MHz, $CDCl_3$, ppm): *δ* 10.01 (s, 1H), 9.01–7.28 (m, 8H), 6.09 (s, 2H), 4.87–4.89 (d, *J* = 6.4Hz, 2H), 4.37–4.35 (d, *J* = 6.8Hz, 2H), 1.40 (s, 3H) ^{13}C NMR (100MHz, $CDCl_3$, ppm): *δ* 168.6, 156.5, 151.3, 149.9, 149.7, 146.2, 138.6, 128.9, 127.8, 127.1, 114.9, 106.7, 104.4, 101.9, 60.7, 52.5, 14.3.

Ethyl 8-((4-(benzyloxy)phenyl)amino)-[1,3]dioxolo[4,5-g]quinoline-7-carboxylate 4

A yellowish solid (1.2 g, 70.0%): ^{1}H NMR (400MHz, $CDCl_3$, ppm): *δ* 10.50 (s, 1H), 9.10 (s, 1H)，7.74–7.28 (m, 6H), 7.01–6.90 (m, 5H), 6.02 (s, 2H), 5.08 (s, 2H), 4.44–4.42 (t, *J* = 6.8Hz, 2H), 1.47–1.44 (t, *J* = 7.2Hz, 3H). ^{13}C NMR (100MHz, $CDCl_3$, ppm): *δ* 168.5, 152.3, 151.6, 149.0, 146.1, 136.8, 135.8, 128.6, 128.0, 127.5, 124.1, 115.7, 115.1, 106.1, 102.7, 101.9, 70.4, 61.1, 50.4, 14.3.

General Procedure for the Synthesis of 5-12.

Excess of iodoalkane (5.0 equiv.) was slowly added to a dry acetonitrile (5 mL) solution of compound 7-(ethoxycarbonyl)-8-(arylamino)-[1,3]dioxolo[4,5-g]quinoline (1.0 equiv.) in seal tube, and was stirred for 2–4 h. The precipeted solide was filtered, to produce the correspondence compound **5~12**.

7-(ethoxycarbonyl)-5-methyl-8-(phenethylamino)-[1,3]dioxolo[4,5-g]quinolin-5-ium iodide 5

A yellow solid (0.38 g, 90%) yield. IR (KBr pellet, cm^{-1}): *v* (N^+) 1483 (strong br). ^{1}H NMR (400MHz, $CDCl_3$, ppm): *δ* 10.35 (d, *J* = 1.2Hz, 1H), 9.16 (s, 1H), 7.73 (s, 1H), 7.42 (s, 1H), 7.36–7.29 (m, 5H), 6.28 (s, 2H), 4.47-4.41 (m, 2H), 4.32 (s, 3H), 4.17-4.16 (t, *J* = 2Hz, 2H), 3.16-3.12 (t, *J* = 6.8 Hz, 7.2Hz，2H), 1.48-1.44 (t, *J* = 7.2 Hz, 3H). ^{13}C NMR (100MHz, $CDCl_3$, ppm): *δ* 166.0, 157.1, 154.9, 148.0, 147.5, 138.9, 136.7, 129.0, 128.9, 127.2, 114.2, 104.2, 102.6, 97.7, 97.7, 62.7, 54.2, 50.7, 44.9, 14.3 HR-MS (FAB) calcd for $C_{22}H_{23}IN_2O_4$ (M^+- I^-) *m/z* 379.1652, observed 379.1659. Calcd for $C_{22}H_{23}IN_2O_4$: C, 52.19; H, 4.58; N, 5.53. Found: C, 52.25; H, 4.61; N, 5.52.

8-((3,4-dimethoxyphenethyl)amino)-7-(ethoxycarbonyl)-5-methyl-[1,3]dioxolo[4,5-g]quinolin-5-ium iodide 6

A yellow solid (0.38 g, 94%) yield. IR (KBr pellet, cm^{-1}): *v* (N^+) 1476 (strong br). ^{1}H NMR (400MHz, $CDCl_3$, ppm): *δ* 10.36 (s, 1H), 9.16 (s, 1H), 7.76 (s, 1H), 7.41 (s, 1H), 6.89–6.85 (m, 3H), 6.28 (s, 2H), 4.45 (m, 2H), 4.17 (s, 2H), 3.90 (s, 3H), 3.87 (s, 3H), 3.11–3.07 (t, *J* = 6.4Hz, 6.8Hz, 2H), 1.49–1.45 (t, *J* = 7.2Hz, 3H). ^{13}C NMR (100MHz, $CDCl_3$, ppm): *δ* 166.0, 154.9, 149.1, 148.2, 148.0, 147.4, 138.9, 135.8, 129.3, 121.0, 114.2, 112.5, 111.6, 104.5, 104.2, 102.4, 97.7, 62.7, 56.0, 56.0, 54.2, 51.2, 45.0, 14.3. HR-MS (FAB) calcd for $C_{24}H_{27}IN_2O_6$ (M^+- I^-) *m/z* 439.1864, observed 439.1859. Calcd for $C_{24}H_{27}IN_2O_6$: C, 50.89; H, 4.81; N, 4.95. Found: C, 50.85; H, 4.82; N, 4.84.

8-(benzylamino)-7-(ethoxycarbonyl)-5-methyl-[1,3]dioxolo[4,5-g]quinolin-5-ium iodide 7

A yellow solid (0.2 g, 48%) yield. IR (KBr pellet, cm^{-1}): *v* (N^+) 1481 (strong br). ^{1}H NMR (400MHz, $CDCl_3$, ppm): *δ* 10.66 (s, 1H), 9.25(s, 1H) 7.78(d, *J* = 1.6Hz, 1H), 7.46–7.39 (m, 6H), 6.28 (s, 2H), 5.11–5.10 (d, *J* = 5.6Hz, 2H), 4.43–4.37 (t, *J* = 7.2Hz, 5H), 1.47–1.43 (t, *J* = 7.2Hz, 3H). ^{13}C NMR (100MHz, $CDCl_3$, ppm): *δ* 165.9, 155.0, 148.2, 147.6, 139.1, 135.5, 129.4, 128.7, 127.5, 116.5, 114.2, 104.4, 104.2, 102.9, 97.8, 62.8, 54.2, 45.0, 14.2. HR-MS (FAB) calcd for $C_{21}H_{21}IN_2O_4$ (M^+- I^-) *m/z* 365.1496, observed 365.1501. Calcd for $C_{21}H_{21}IN_2O_4$: C, 51.23; H, 4.30; N, 5.69. Found: C, 51.22; H, 4.32; N, 5.58.

8-((4-(benzyloxy)phenyl)amino)-7-(ethoxycarbonyl)-5-methyl-[1,3]dioxolo[4,5-g]quinolin-5-ium iodide 8

A yellow solid (0.16 g, 39%) yield. IR (KBr pellet, cm^{-1}): *v* (N^+) 1474 (strong br). ^{1}H NMR (400MHz, $CDCl_3$, ppm): *δ* 11.70 (s, 1H), 9.45(s, 1H), 7.47–7.37(m, 6H), 7.22–7.20(d, *J* = 8.4Hz, 2H), 7.06–7.03 (t, *J* = 8.8Hz, 6Hz, 3H), 6.20 (s, 2H), 5.13 (s, 2H,), 4.51–4.48 (t, *J* = 7.2Hz, 5H), 1.54–1.50 (t, *J* = 6.8Hz, 3H). ^{13}C NMR (100MHz, $CDCl_3$, ppm): *δ* 166.2, 158.4, 155.1, 155.0, 147.9, 147.6, 139.5, 136.2, 131.7, 128.6, 128.2, 127.5, 126.0, 116.5, 114.2, 104.3, 104.0, 103.8, 97.8, 70.4, 63.0, 45.6, 14.4. HR-MS (FAB) calcd for $C_{27}H_{25}IN_2O_5$ (M^+- I^-) *m/z* 457.1758, observed 457.1752. Calcd for $C_{27}H_{25}IN_2O_5$: C, 55.49; H, 4.31; N, 4.79. Found: C, 55.47; H, 4.30; N, 4.74.

7-(ethoxycarbonyl)-8-(phenethylamino)-5-propyl-[1,3]dioxolo[4,5-g]quinolin-5-ium iodide 9

A white powder (0.31 g, 71%) yield. IR (KBr pellet, cm^{-1}): *v* (N^+) 1485 (strong br). ^{1}H NMR (400MHz, $CDCl_3$, ppm): *δ* 10.37-10.37 (d, *J* = 0.4Hz, 1H), 9.21 (s, 1H), 7.76 (s, 1H), 7.39–7.29 (m, 6H), 6.30 (s, 2H), 4.75–4.71 (t, *J* = 7.6Hz, 2H), 4.50–4.44 (m, 2H), 4.21–4.20 (d, *J* = 5.2Hz, 2H), 3.18–3.15 (t, *J* = 7.2Hz, 2H), 2.02–1.97 (m, 2H), 1.51–1.47 (t, *J* = 7.2Hz, 3H), 1.08 (s, 3H). ^{13}C NMR (100MHz, $CDCl_3$, ppm): *δ* 165.9, 157.2, 155.0, 148.0, 146.5, 137.9, 136.7, 128.9, 128.9, 127.2, 114.6, 104.6, 104.3, 102.6, 97.5, 62.8, 58.2, 50.9, 36.5, 22.2, 14.5, 10.9. HR-MS (FAB) calcd for C24H27IN2O4 (M^+- I^-) *m/z* 407.1965, observed 407.1963. Calcd for $C_{24}H_{27}IN_2O_4$: C, 53.94; H, 5.09; N, 5.24. Found: C, 53.92; H, 5.11; N, 5.26.

8-((3,4-dimethoxyphenethyl)amino)-7-(ethoxycarbonyl)-5-propyl-[1,3]dioxolo[4,5-g]quinolin-5-ium iodide 10

A white powder (0.27 g, 63%) yield. IR (KBr pellet, cm^{-1}): *v* (N^+) 1477 (strong br). ^{1}H NMR (400MHz, $CDCl_3$, ppm): *δ* 10.28-10.27 (d, *J* = 0.8Hz, 1H), 9.08 (s, 1H), 7.76 (s, 1H), 7.31 (s, 1H), 6.87 (s, 1H), 6.80-6.79 (d, *J* =

4Hz, 2H), 6.25 (s, 2H), 4.65–4.61 (t, *J* = 7.2Hz, 2H), 4.41–4.36 (m, 2H), 4.17 (s, 2H), 3.85–3.80 (d, *J* = 20Hz, 6H), 3.06–3.03 (t, *J* = 6.0Hz, 2H), 1.93–1.89 (t, *J* = 7.2Hz, 2H), 1.44–1.40 (t, *J* = 7.2Hz, 3H), 1.03–0.99 (t, *J* = 7.2Hz, 3H). ^{13}C NMR (100MHz, $CDCl_3$, ppm): *δ* 165.9, 154.9, 149.1, 148.1, 147.9, 146.5, 137.8, 137.8, 129.2, 121.0, 114.5, 112.5, 111.6, 104.8, 104.3, 102.4, 97.4, 62.7, 58.2, 56.1, 56.0, 51.3, 36.0, 22.2, 14.5, 10.9. HR-MS (FAB) calcd for $C_{26}H_{31}IN_2O_6$ (M^+- I^-) *m/z* 467.2177, observed 467.2174. Calcd for $C_{26}H_{31}IN_2O_6$: C, 52.53; H, 5.26; N, 4.71. Found: C, 52.58; H, 5.19; N, 4.68.

8-(benzylamino)-7-(ethoxycarbonyl)-5-propyl-[1,3]dioxolo[4,5-g]quinolin-5-ium iodide 11

A white powder (0.31 g, 70%) yield. IR (KBr pellet, cm^{-1}): *v* (N^+) 1475 (strong br). ^{1}H NMR (400MHz, $CDCl_3$, ppm): *δ* 10.69 (s, 1H), 9.28–9.27 (t, *J* = 1.2Hz, 1H), 7.84–7.83 (m, 1H), 7.43(s, 6H), 6.29 (s, 2H), 5.14–5.13 (d, *J* = 5.2Hz, 2H), 4.77 (s, 2H), 4.43–4.42 (d, *J* = 6.8Hz, 2H), 2.03–2.02 (d, *J* = 7.2Hz, 2H), 1.48–1.44 (t, *J* = 7.2Hz, 3H), 1.12–1.08 (t, *J* = 7.2Hz, 3H). ^{13}C NMR (100MHz, $CDCl_3$, ppm): *δ* 165.8, 155.1, 148.1, 146.6, 137.9, 135.5, 129.3, 128.6, 127.4, 114.6, 104.7, 104.2, 103.0, 100.0, 97.5, 62.8, 58.2, 53.6, 22.2, 14.4, 10.9. HR-MS (FAB) calcd for $C_{23}H_{25}IN_2O_4$ (M^+- I^-) *m/z* 393.1809, observed 393.1807. Calcd for $C_{23}H_{25}IN_2O_4$: C, 53.09; H, 4.84; N, 5.38. Found: C, 53.12; H, 4.83; N, 5.39.

8-((4-(benzyloxy)phenyl)amino)-7-(ethoxycarbonyl)-5-propyl-[1,3]dioxolo[4,5-g]quinolin-5-ium iodide 12

A white powder (0.32 g, 77%) yield. IR (KBr pellet, cm^{-1}): *v* (N^+) 1474 (strong br). ^{1}H NMR (400MHz, $CDCl_3$, ppm): *δ* 11.59 (s, 1H), 9.38 (s, 1H), 7.39–7.28 (m, 6H), 7.15–7.14 (d, *J* = 6.8Hz, 2H), 7.12–7.00 (d, *J* = 8.8Hz, 3H), 6.18 (s, 2H), 5.06 (s, 2H), 4.78 (s, 2H), 4.44–4.43 (d, *J* = 4.8Hz, 2H), 2.01 (s, 2H), 1.47–1.46 (d, *J* = 4Hz, 3H), 1.08–1.07 (d, *J* = 3.2Hz, 3H). ^{13}C NMR (100MHz, $CDCl_3$, ppm): *δ* 166.2, 158.4, 155.2, 154.7, 147.6, 138.4, 136.2, 131.5, 128.6, 128.2, 127.5, 126.0, 116.5, 114.5, 104.5, 104.2, 103.8, 97.5, 70.4, 63.1, 58.6, 22.5, 14.5, 11.0. HR-MS (FAB) calcd for $C_{29}H_{29}IN_2O_5$ (M^+- I^-) *m/z* 485.2071, observed 485.2064. Calcd for $C_{29}H_{29}IN_2O_5$: C, 56.87; H, 4.77; N, 4.57. Found: C, 56.85; H, 4.72; N, 4.56.

In vitro cytotoxicity

The three cancer cell lines (A549, SGC-7901, and Hela) and normal cell lines (normal liver L-02 cells and normal lung IMR 90 cells), were acquired from the American Type Culture Collection (Manassas, VA, USA). A549 and SGC-7901 cells were cultured routinely in RPMI-1640, and Hela and L-02 cells were cultured routinely in DMEM. The medium was supplemented with 10% fetal bovine serum (FBS). The cells were maintained at sub-confluence at 37°C in humidified air containing 5% CO_2. The cells were monitored daily and maintained at an 80% cell density.

The cytotoxicity of the tested samples was measured against each cell line using the MTT Cell Viability Cancer cells (A549, SGC-7901 and Hela) and normal human cells lines (liver L-02 cells and lung IMR 90 cells) were harvested during the logarithmic phase of growth. All the cells were seeded in 96-well plates at 10^4 cells/well and then treated with various concentrations (1, 3, 10, 30, or 100 μmol/mL) of 5-FU, methotrexate and the tested samples for 24 h. The MTT solution (20 μL; 5 mg/mL) was added to each well, and the cells were cultured for 4 h at 37°C. The supernatants were removed, and resolved with 100 μL of DMSO, and the cells were shocked for 10 min. The optical density of the samples was measured at 490 nm on a microplate luminometer. The cell viability is expressed as the percentage change in absorbance compared to the control values.

In vitro antimicrobial evaluation

The synthetic compounds **1~12** against two bacterial strains were measured using the broth microdilution method in 96-well plates, and the MIC values were determined. The MIC is defined as the lowest concentration of test sequences that completely inhibit growth. The microorganisms used in the present study were *S. aureus* (ATCC 29213) and *E. coli* (ATCC 8739). This was placed on the inoculated muller-Hinton agar plates, and the test compounds were dissolved in DMSO to obtain final concentrations of 1-50 nmol • mL^{-1}. The final bacterial concentration was approximately 10^6 CFU mL^{-1}. The MIC values were measured after incubation for 24 h at 37 °C. Ciprofloxacin and amoxicillin were used as controls and assayed under identical conditions. All experiments were performed in triplicate.

Molecular docking

AutoDock Vina software package version 1.1.2 was used to perform docking simulations. The target 3D crystal structure of human topoisomerase I and *S. aureus* DNA gyrase (Topo II) in Protein Data Bank (PDB) were downloard (PDB ID: 1TL8, 2XCT) and prepared for docking using the docking program AutoDockVina 1.1.2. and MGLTools. The docking result was analyzed and optimized by Pymol 1.5.6.

Acknowledgements

This study was supported financially by the scientific research foundation of Jiangsu University (Grant No. 5501290005).

Conflict of Interest statement

The authors declare no conflict of interest.

Keywords: quinoline and quinolinium iodide • anticancer • antibacterial • human cancer • human bacterial strains

References:

[1] J. Wang, Y. Yao, X. Chen, J. Wu, T. Gu, X. Tang, *Biomed. Pharmacother.* **2018**, *108*, 1451-1459.
[2] D. Zhou, J. Jin, Q. Liu, J. Shi, Y. Hou, *Eur. J. Pharmacol.* **2019**, *842*, 248-254.
[3] H. Shen, F. Li, D. Wang, *Drug Des. Devel. Ther.* **2018**, *12*, 921-934.
[4] X. -q. Li, J. Ren, P. Chen, *Acta Pharmacol. Sin.* **2018**, *39*, 1359-1372.
[5] M. Kadela-Tomanek, E. Bebenek, E. Chrobak, *Eur. J. Med. Chem.* **2019**, *177*, 302-315.
[6] H. Zhang, G. K. Mahunu, R. Castoria, Q. Yang, M. T. Apaliya, *Trends Food Sci. Technol.* **2018**, *78*, 180-187.
[7] H. Zhang, W. Xu, E. Omari-Siaw, *Drug Delivery* **2017**, *24*, 1170-1178.
[8] G. Wang, X. -L. Fu, J. -J. Wang, R. Guan, X. -J. Tang, *Curr. Cancer Drug Targets* **2017**, *17,* 17-39.

[9] J. Hou, E. Sun, Z. -H. Zhang, *Drug Delivery* **2017**, *24*, 261-269.
[10] M. Jiang, H. Y. Lu, X. H. Shan, *Eur. Rev. Med. Pharmacol. Sci.* **2018**, *22*, 4146-4155.
[11] H. Ding, J. Wang, F. P. Jia, J. Yi, M. Zhang, *Eur. Rev. Med. Pharmacol. Sci.* **2017**, *21*, 3218-3222.
[12] J. -Y. Wan, H. Yao, *J. Appl. Biomed.* **2018**, *16*, 311-319.
[13] T. Liu, T. Yu, H. Hu, K. He, *Biomed. Pharmacother.* **2018**, *98*, 286-296.
[14] Y. Wen, J. -H. Yuan, Q. -Y. Zhou, W. -B. Wang, X. -F. Xu, Int. J. Agric. Biol. **2019**, *22*, 769-773.
[15] A. Mrozek-Wilczkiewicz, K. Malarz, M. Rejmund, J. Polanski, R. Musiol, *Eur. J. Med. Chem.* **2019**, *171*, 180-194.
[16] D. B. Yaakov, Y. Shadkchan, N. Albert, D. P. Kontoyiannis, N. Osherov, *J. Antimicrob. Chemother.* **2017**, *72*, 2263-2272.
[17] M. Szumilak, M. Galdyszynska, K. Dominska, A. Stanczak, *Acta Biochim. Pol.* **2017**, *64*, 307-313.
[18] N. Kotecki, A. Gombos, A. Awada, *Expert Rev. Anticancer Ther.* **2019**, *19*, 447-454.
[19] K. Zhang, R. Hong, L. Kaping, *Cancer Lett. (N. Y., NY, U. S.)* **2019**, *447*, 130-140.
[20] K. T. Santoso, A. Menorca, C-Y. Cheung, G. M. Cook, B. L. Stocker, M. S. M. Timmer, *Bioorg. Med. Chem.* **2019**, *27*, 3532-3545.
[21] H. Zhan, X. Zhou, Y. Cao, T. Jagtiani, T. -L. Chang, J. F. Liang, *J. Mater. Chem. B* **2017**, *5*, 2692-2701.
[22] N. M. Khalifa, M. A. Al-Omar, A. A. Abd El-Galil, M. Abd El-Reheem, *Biomed. Res. (Aligarh, India)* **2017**, *28*, 869-874.
[23] J. Olatunji, H. Chen, Y. Zhou, *Biomed. Pharmacother.* **2018**, *102*,1145-1151.
[24] X. Hu, L. Yuan, L. Han, S. Li, L. Song, *RSC Adv.* **2019**, *9*, 27449-27454.
[25] E. Fokum, H. M. Zabed, Q. Guo, J. Yun, M. Yang, H. Pang, Y. An, W. Li, X. Qi, *Food Biosci.* **2019**, *28*, 125-132.
[26] A. H. Romero, *Top. Curr. Chem.* **2019**, *377*, 1-22.
[27] Ansari, A. Ali, M. Asif, *Steroids* **2019**, *148*, 99-113.
[28] T. Y. Senbadejo, O. E. Fagade, *Fountain J. Nat. Appl. Sci.* **2017**, *6*, 9-14.
[29] D. Painuly, S. Y. Mullemwar, M. E. Rabanal, R. Singhal, I. M. Nagpure, *Appl. Phys. A: Mater. Sci. Process.* **2019**, *125*,1-10.
[30] J. J. Krishnan, A. Gangaprasad, K. Satheeshkumar, *Ind. Crops Prod.* **2018**, *119*, 93-101.
[31] Y. B. Chong, D. W. Sun, X. Zhang, C. Y. Yue, J. L. Yang, *Chemical Engineering Journal* **2019**, *372*, 496-508.
[32] A. Mrozek-Wilczkiewicz, M. Kuczak, K. Malarz, W. Cieslik, E. Spaczynska, R. Musiol, *Eur. J. Med. Chem.* **2019**, *177*, 338-349.
[33] T. Su, J. Zhu, R. Sun, *Eur. J. Med. Chem.* **2019**, *178*, 154-167.
[34] N. Chokkar, S. Kalra, M. Chauhan, R. Kumar, *Mini-Rev. Med. Chem.* **2019**, *19*, 510-526.
[35] J. Fedorowicz, J. Saczewski, A. Konopacka, *Eur. J. Med. Chem.* **2019**, *179*, 576-590.
[36] J. Wang, C. Zhao, J. Tu, *J. Biomol. Struct. Dyn.* **2019**, *37*, 2913-2925.
[37] A. Carta, A. Bua, P. Corona, *Eur. J. Med. Chem.* **2019**, *161*, 399-415.
[38] S. Sreenivasa, G. Shivaraja, V. Chandramohan, T. M. C. Rao, *J. Appl. Chem. (Lumami, India)* **2018**, *7*, 1606-1616.
[39] R. Niu, Y. Yang, Y. Wang, S. Luo, C. Zhang, Y. Wang, *Food Sci. Technol.* **2019**, *39*, 500-506.
[40] Y. Feng, Y. Zhu, J. Wan, X. Yang, C. K. Firempong, J. Yu, X. Xu, *J. Funct. Foods* **2018**, *44*, 137-145.
[41] J. Szczepaniak, W. Cieslik, A. Romanowicz, R. Musiol, A. Krasowska, *Int. J. Antimicrob. Agents* **2017**, *50*, 171-176.
[42] R. Musiol, *Expert Opin. Drug Discovery* **2017**, *12*, 583-597.
[43] Douara, M. Manachou, N. Merabet, S. Boughdiri, L. Belkhiri, *J. Mol. Struct.* **2019**, *1193*, 416-428.
[44] M. E. Haiba, E. S. Al-Abdullah, N. S. Ahmed, H. A. Ghabbour, H. M. Awad, *J. Mol. Struct.* **2019**, *1195*, 702-711.
[45] R. E. Karmis, S. Carrara, A, A, Baxter, C. F. Hogan, M. D. Hulett, P. J. Barnard, *Dalton Trans.* **2019**, *48*, 9998-10010.
[46] M. C. Pfrunder, A. J. Brock, A. S. Micallef, J. K. Clegg, J. McMurtrie, *Cryst. Growth Des.* **2019**, *19*, 5334-5342.
[47] R. D. Larsen, D. Cai, *Sci. Synth.* **2005**, 15, 389-549.
[48] Z. Zhou, M. Tang, Y. Liu, Z. Zhang, R. Lu, J. Lu, *Anti-Cancer Drugs* **2017**, *28*, 446-456.
[49] T. Wu, J. Geng, W. Guo, J. Gao, X. Zhu, *Acta Pharm. Sin. B* **2017**, *7*, 65-72.
[50] W. Wang, B. Zhang, A. M. Mani, *J. Pharmacol. Exp. Ther.* **2018**, *366*, 184-193.
[51] J. Xu, J. Zheng, Z. Zhou, X. Han, *Trop. J. Pharm. Res.* **2018** ,*17*, 681-686.
[52] L. Ruan, Y. Shen, Z. Lu, *Clin. Exp. Pharmacol. Physiol.* **2017**, *44*, 909-913.
[53] L. Yang, Z. Zhang, J. Hou, *Int. J. Nanomed.* **2017**, *12*, 7653-7667.
[54] S. W. Kim, J. H. Kim, S. N. Kim, D. P. Kang, Y. H. Han, G. F. Jin, D. S. Jung, S. H. Park, J. M. Kim, J. Zheng, (Oscotec INC, Tian'an City, Korea) Korea pat. WO 2011132967A2, **2011**.
[55] R. Wang, K. Xu, W. X. Shi, *Arch. Pharm. (Weinheim, Ger.)* **2019**, *352*, 1900045.
[56] E. R. Pereira, T. P. Resende, E. Vasquez, L. Marshall-Lund, R. M. C. Guedes, C. J. Gebhart, *Equine Veterinary Journal* **2019**, *51*, 665-668.
[57] T. Oleg, A. J. Olson, *J. Comput. Chem.* **2010**, *31*, 455-461.
[58] S. K. Arepalli, C. Lee, S. Sim, *Bioorg. Med. Chem.* **2018**, *26*, 5181-5193.
[59] R. G. Gouveia, A. G. Ribeiro, M. A. Santos Pinheiro Segundo, *Bioorg. Med. Chem.* **2018**, *26*, 5911-5921.
[60] S. Murugavel, C. Ravikumar, G. Jaabil, P. Alagusundaram, *Comput. Biol. Chem.* **2019**, *79*, 73-82.
[61] A. Ioanoviciu, S. Antony, Y. Pommier, B. L. Staker, L. Stewart, M. Cushman, *J. Med. Chem.* **2005**, *48*, 4803-4814.
[62] B. D. Bax, P. F. Chan, D. S. Eggleston, *Nature* **2010**, *466*, 935-940.

Entry for the Table of Contents

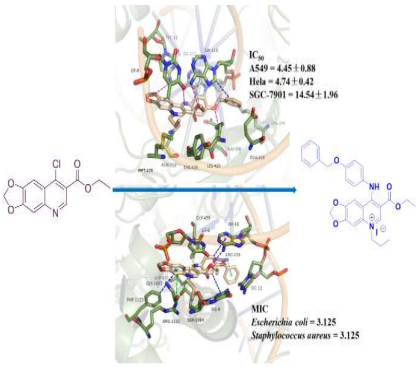

We prepared a series of novel quinoline and quinolinium iodide derivatives starting from Ethyl 8-chloro-[1,3]dioxolo[4,5-g]quinoline-7-carboxylate and the arylamine compounds to discover potential anticancer and antibacterial agents. The target compounds 12 was found to be the most potent derivative with IC50 values, stronger than the positive control 5-FU and MTX. Furthermore, compound 12 had the most potent inhibitory activity. The MIC of this compound against test cells were 3.125 nmol·mL-1, which was smaller than that of the reference agents, amoxicillin and ciprofloxacin.